Nanoscale Res Lett (2008) 3:260–264
DOI 10.1007/s11671-008-9148-y

NANO EXPRESS

Preparation and Properties of ε-Fe_3N-Based Magnetic Fluid

Wei Huang · Xiaolei Wang

Received: 17 May 2008 / Accepted: 11 July 2008 / Published online: 25 July 2008

Abstract In this work, ε-Fe_3N nanoparticles and ε-Fe_3N-based magnetic fluid were synthesized by chemical reaction of iron carbonyl and ammonia gas. The size of ε-Fe_3N nanoparticles was tested by TEM and XRD. Stable ε-Fe_3N-based magnetic fluid was prepared by controlling the proper ratio of carrier liquid and surfactant. The saturation magnetization of stable ε-Fe_3N-based magnetic fluid was calculated according to the volume fraction of the particles in the fluid. The result shows that both the calculated and measured magnetizations increase by increasing the particle concentration. With the increasing concentration of the ε-Fe_3N particles, the measured value of the magnetic fluid magnetization gradually departs from the calculated magnetization, which was caused by agglomeration affects due to large volume fraction and large particle size.

Keywords Iron nitrides · Magnetic fluids · X-ray diffraction · Magnetic properties

Introduction

Magnetic fluids or ferrofluids, are comprised of magnetic nanoparticles stabilized by coating surfactants and dispersed in various media, most notably hydrocarbons, esters or water [1–5]. The stability of magnetic fluid depends upon a balance between repulsive and attractive interactions among nanoparticles [6]. Besides the thermal motion, the steric and electrostatic repulsive interactions are against Van der Waals and dipolar attractive interactions [7]. The magnetic properties of magnetic fluids depend strongly on the size of the particles and the concentration of the magnetic material in the dispersion. In the presence of a magnetic field, the magnetic moment of the particles will try to align with the magnetic field direction leading to a macroscopic magnetization of the fluid. When the external field is removed, the particles quickly randomize the directions of their magnetic moment and the fluid loses its magnetism.

The study and application of magnetic fluids were invented in the mid-1960s, involving the multidisciplinary sciences such as chemistry, fluid mechanics, and magnetism. With modern advances in understanding nanoscale systems, current research focuses on synthesis, characterization, and functionalization of magnetic fluids. Iron oxide fluids in hydrophobic media are now used industrially for rotating shaft seals, loudspeaker coils, and in various magnetically promoted separations [8].

However, the magnetic properties of iron oxide-based fluids are not sufficient for a number of purposes. Many efforts have been devoted to make magnetic fluid with higher magnetization. A variety of techniques have been developed to fabricate magnetic fluid using metal particles such as spark erosion [9] and vacuum evaporation [10]. One of the major difficulties encountered is that the magnetization of the metal particles decays with time, due to the lack of oxidization resistance in the ambient environment. According to Nakatani et al. [11], the iron-nitride compounds are ferromagnetic with higher magnetization than iron oxide (Fe_3O_4) and are chemically stable. They are

W. Huang (✉) · X. Wang
Jiangsu Key Laboratory of Precision & Micro-manufacturing Technology, Nanjing University of Aeronautics & Astronautics, Nanjing 210016, China
e-mail: 5543837@sina.com

W. Huang
Department of Functional Material Research, Central Iron & Steel Research Institute, Beijing 100081, People's Republic of China

metallic with a close packed lattice of iron atoms whose interstices are occupied by nitrogen atoms. It is considered that there exists covalent bonding between the iron atoms and the nitrogen atoms. Thus, fine particles of ferromagnetic iron-nitrides have a potential application to magnetic fluids that need a high magnetization and stability against oxidation.

In this article, single-phase ε-Fe_3N-based magnetic fluid and nanometer powders were analyzed. In the magnetic fluids, the nanosized ε-Fe_3N powders coated by surfactants were dispersed in carrier liquid. The assays performed for the preparation, stability, and evaluation of the magnetic fluids are discussed in the following sections.

Experimental Procedures

Iron-nitride-based magnetic fluid was synthesized according to the method reported in Ref. [12]. The carrier liquid was composed of 80-mL α-olefinic hydrocarbon synthetic oil (PAO4 oil with low volatility and low viscosity) and a certain amount of succinicimide (surfactant) (see Table 1). The iron-nitride nanometer powder can also be synthesized using the same method. The only difference is that the carrier liquid used in powder preparation was synthetic oil without any surfactant. It is convenient to collect the dried particles when they are not coated by surfactant using a magnet. The reaction temperature of the synthetic oil was strictly controlled at 182 °C. The gas flux ratio was fixed at Ar1:Ar2:NH_3 = 7:2:2 where Ar1 and Ar2 represent argon gas coming from two gas pipes according to the Ref. [12]. The argon gas Ar1 was used to carry the iron carbonyl which was heated to gasify at 37.5 °C. The argon gas Ar2 was used to control the concentration of iron carbonyl vapor and ammonia gas in the mixed gas. The pore size range of the porous plate used is 20–30 μm [12].

X'Pert PRO (Panalytical) X-ray diffractometer was used to analyze the phase composition of magnetic particles. The diffraction was performed with $Co_{k\alpha 1}$ (λ = 1.7889 Å) and the ray was filtered by the graphite. The experimental parameters used were: 40 mA, 35 kV, continuous scan, scan speed 2°/min. Particle sizes of iron-nitride coated with surfactant were measured with a 2,100 fx transmission electron microscope (TEM) operated at 200 keV. TEM samples were prepared by dispersing the particles in alcohol using ultrasonic excitation, and then transferring the nanoparticles on the carbon films supported by copper grids. The density of the magnetic fluid was measured using a picnometer at 20 ± 1 °C. The sedimentation stability of the magnetic fluid was evaluated by changing the ratio of the synthetic oil (PAO4) and surfactant. After obtaining stable magnetic fluid, the magnetic properties of the magnetic powders and the magnetic fluids were measured immediately after preparation using a LDJ9500 vibrating sample magnetometer (VSM). Samples were contained in a small glass cup with internal dimensions of 2 × 2 × 2 mm^3, which were sealed by gluing a small cover glass over the open end. Then the glass cup was put in the magnetic uniform area of the pole. The hysteresis curve was recorded per 1.5 s. All measurements were performed at room temperature. The relationship between the calculated/measured saturation magnetization and particle content is also discussed.

Table 1 The surfactant content in five magnetic samples (FN001–FN005)

No.	FN001	FN002	FN003	FN004	FN005
Carrier (PAO4) mL	80	80	80	80	80
Surfactant (succinamide) mL	5	10	15	20	25

Results and Discussion

Phase Structure and Particle Size

Diffraction pattern of the powders dried in vacuum is shown in Fig. 1. Each of the diffraction peaks shown in Fig. 1 represents different crystal plane orientation of the ε-Fe_3N particles. From Fig. 1, we can see that the sites and intensity of the diffraction peaks are consistent with the standard pattern for ε-Fe_3N (JCPD No.1-1236) but it is obvious that every peak is broadened. According to the Scherrer relationship, $d_{hkl} = 0.9\lambda/B\cos\theta$ (B is the half width of XRD diffraction lines, λ = 1.7889 Å, θ is the half diffraction angle of 2θ), particle size was calculated. In this equation the contribution to broadening by internal strains and imperfections is not accounted. The average particle size d_{hkl} was determined by taking an average particle size

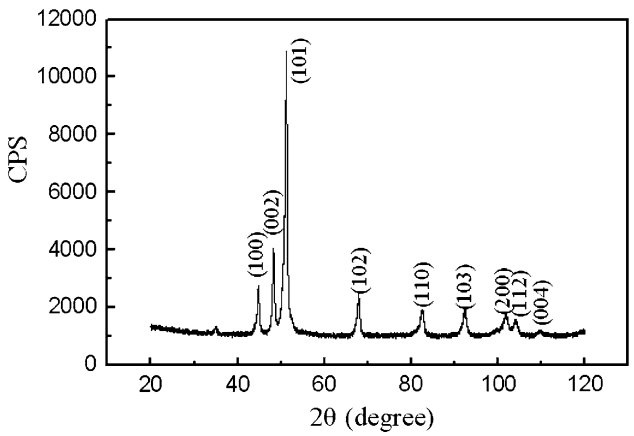

Fig. 1 X-ray diffraction pattern of ε-Fe_3N magnetic particle ($Co_{k\alpha 1}$)

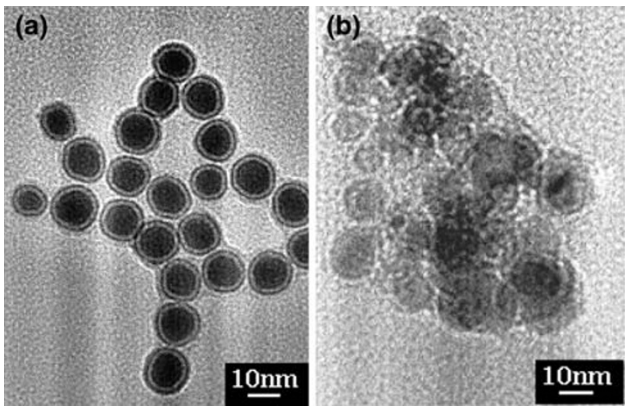

Fig. 2 TEM image of ε-Fe_3N nanoparticles. (**a**) Coated with surfactant, (**b**) without any surfactant

of d_{002}, d_{101}, d_{102}, and the average particle size of 18.9 ± 2 nm is obtained.

Figure 2a shows TEM images of ε-Fe_3N particles covered with surfactant. It can be seen that the ε-Fe_3N particles synthesized in our experiment are spherical and have very narrow size distributions. Every particle is covered completely by the surfactant and dispersed in the carrier liquid homogeneously. The average particle size is about 21 ± 1 nm which approximate the sizes calculated by the Scherrer formula. Figure 2b gives the TEM images of ε-Fe_3N particles without any surfactant. It is known that uncovered nanoparticles are easy to agglomerate for the high surface energy. Particles in Fig. 2b are not covered with a surfactant and they formed an agglomerate structure which caused the image in Fig. 2b to be fuzzy compared with Fig. 2a. The particles appear as clusters with average particle size of 23 ± 2 nm which are larger than the particles coated with surfactant. Since the carrier liquid is only 100 mL α-olefinic hydrocarbon synthetic oil, the ε-Fe_3N particles cannot be covered by surfactant and the particle's collisions lead to the formation of larger magnetic particles. As ε-Fe_3N nanoparticles are ferromagnetic, one possible explanation of the difference between calculated value from XRD and observed particle size is due to particle aggregation under the influence of the electromagnetic field in the TEM [13] while X-ray line broadening analysis discloses the size of the primary particles. Compared with the two TEM images, we can see that the ε-Fe_3N particles could be dispersed as single particles in α-olefinic hydrocarbon synthetic oil with the aid of succinicimide as surfactant.

The Stability of the Magnetic Fluids

The stability is one of the most important properties for magnetic fluid and it will strongly affect the service life. The well-known magnetite magnetic fluids have a good stability. Here the stability of ε-Fe_3N-based magnetic fluid was investigated.

In this part, five ε-Fe_3N magnetic fluid samples were prepared and all the reaction conditions were the same except the content of the surfactant in the carrier liquid given in Table 1.

After preparation, the initial density of the five magnetic fluid (ρ_{ini}) samples was measured. Resting all the magnetic fluid samples above in a tube for a period of time, we then move 0.9 volume of the fluid to the top of the tube. ρ_{bot} represents the density of the fluid in the bottom one tenth of the tube after resting for a period of time. The smaller variation of the density$(\rho_{bot} - \rho_{ini})$, the more stable the fluid is. Then the stability of the fluids was roughly estimated from the percentage of particles suspended and it was calculated as Eq. 1:

$$S\% = \left(1 - \frac{\rho_{bot} - \rho_{ini}}{\rho_{ini}}\right) \times 100\% \quad (1)$$

where $S\%$ expresses the suspension percentage of the magnetic particles in fluid.

After resting for 30 days, ρ_{bot} of the five magnetic fluids with different surfactant were measured. The particle suspension percentage ($S\%$) of the five magnetic fluid samples was obtained using Eq. 1 and the relationships between $S\%$ and surfactant content in the carrier liquid are given in Fig. 3. From Fig. 3 we can see that suspension percentage ($S\%$) increases with the increase of surfactant content. When the volume fraction of the surfactant in carrier liquid reaches 20%, the $S\%$ calculated by Eq. 1 becomes the maximum value (97%). It slightly decreases to 95% when the volume fraction of the surfactant reaches 23.8% and this may be caused by measurement error. According to Eq. 1, the suspension percentage of samples FN001–FN003 is lower and is due to the higher value of ρ_{bot}. This means that the particles cannot be coated completely by the surfactant due to the deficiency of surfactant content and

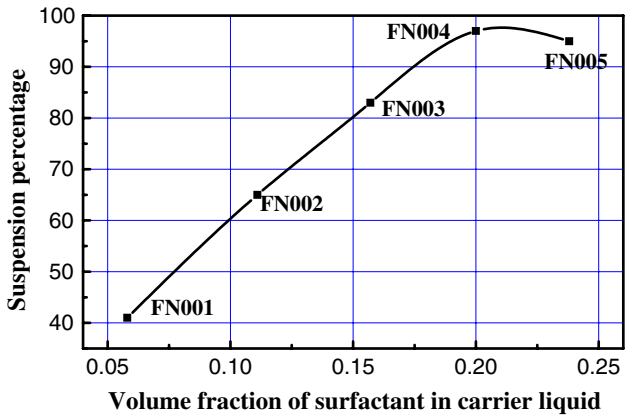

Fig. 3 The relationship between the stability of magnetic fluid related to suspension percentage of Eq. 1 and surfactant amounts

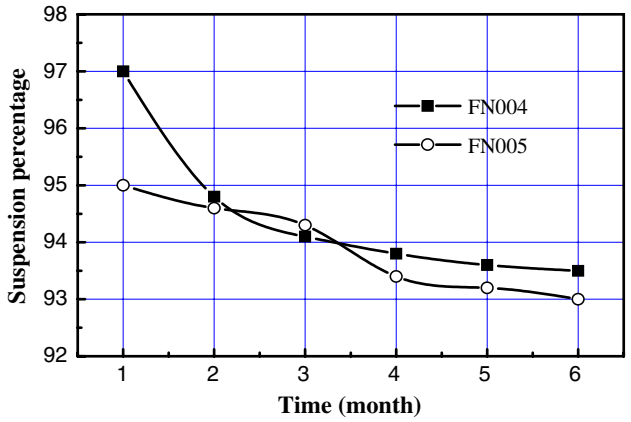

Fig. 4 The relationship between suspension percentage and resting time

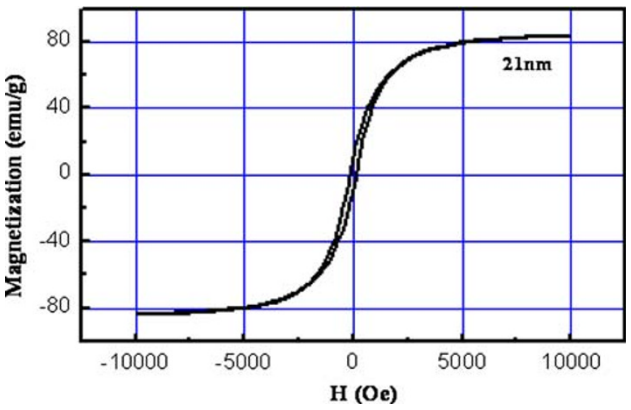

Fig. 5 Hysteresis loops at room temperature of the ε-Fe_3N nanoparticles under the field up to 10 kOe (σ_s = 83.5 emu/g)

part of them have settled to the bottom of the tube. When the volume ratio of surfactant was in the range of 20–23.8% (samples FN004 and FN005), the suspension percentage is higher. This means that the magnetic particles can be coated completely by the surfactant and dispersed in the carrier liquid homogeneously (see Fig. 2a).

The stability of samples FN004 and FN005 versus time is given in Fig. 4. It can be seen that suspension percentage of the two samples decreases quickly in the first 4 months. It then changes slowly with resting time. After resting for 6 months the changes of *S*% for samples FN004 and FN005 are 3.5% and 2.0%, respectively. Both of the suspension percentages of samples FN004 and FN005 are kept above 92% calculated using Eq. 1 after 6 months and they can be considered stable.

Magnetic Properties

In this part, five stable ε-Fe_3N magnetic fluids with different particle content were prepared using 80-mL synthetic oil (PAO4) and 20-mL surfactant. Pure ε-Fe_3N particles were also prepared using synthetic oil (PAO4) only.

Figure 5 exhibits the room temperature hysteresis loops of pure ε-Fe_3N nanoparticles samples under the field up to 10 kOe. Though the 10-kOe field may not be high enough to saturate the sample, the powder sample approaches to saturation and the value is about 83.5 emu/g, which can be considered as the saturation magnetization (σ_s). In Fig. 5 we can see that there is a small amount of hysteresis loss in the curve and this may be caused by the size of the particles. For the particles with no surfactant during preparation, the size of part of the particles in the powder sample is larger than the single domain dimension which will show some ferromagnetic loss. The coercivity value (*Hc*) of the particles was measured to be 129 Oe. According to Viota et al. [14], the volume fraction (Φ) of a solid phase in magnetic fluid can be obtained by measuring the magnetic fluid density (ρ). The density of the fluid can be expressed as Eq. 2:

$$\rho = \rho_S \Phi + \rho_f (1 - \Phi) \tag{2}$$

where ρ_f (0.84 g/cm^3) is the density of the liquid phase and ρ_s(6.88 g/cm^3) is the density of solid phase. Then the volume fraction (Φ) of the solid phase in magnetic fluid is

$$\Phi = \frac{\rho - \rho_f}{\rho_S - \rho_f} \tag{3}$$

If the interaction between magnetic particles in a certain magnetic fluid is ignored, the saturation magnetization of a magnetic fluid should be considered as the sum of the magnetization of all the dispersed magnetic particles. Taking the density (ρ) as a variable, the value of the saturation magnetization (emu/g) for magnetic fluids can be expressed as:

$$\sigma = \rho_S \frac{\sigma_S}{\rho} \left(\frac{\rho - \rho_f}{\rho_S - \rho_f} \right) \tag{4}$$

where σ_s and σ are the magnetization of the dispersed particles and magnetic fluid, respectively.

Figure 6 gives the relations between the calculated volume fraction (Φ) of particles and the density of the magnetic fluid samples using Eq. 3. It can be noticed that the density of the fluid increases linearly with increasing Φ of iron-nitride magnetic particles in the fluid. The measured magnetization and the calculated values using Eq. 4 for the different volume fractions of the ε-Fe_3N-based magnetic fluids are also shown in Fig. 6. It can be seen that both the calculated and measured magnetizations increase with increasing Φ of the particles in the fluid. At the low concentrations, the measured values are close to the calculated one. With the increasing volume fraction of the ε-Fe_3N particles, the measured values gradually depart from the calculated magnetizations. The phenomenon may be caused by two reasons: (1) particle volume fraction, (2) particle size. In magnetic fluid, in addition to the

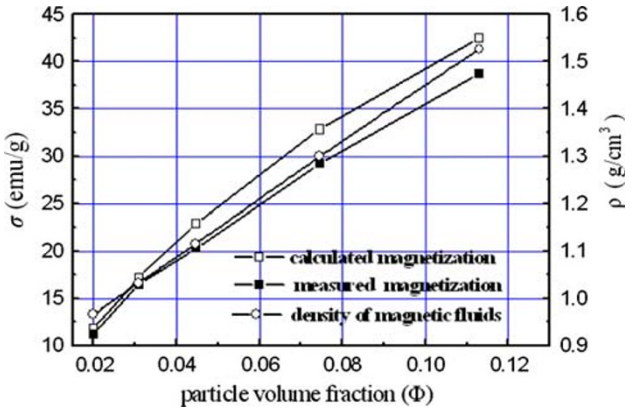

Fig. 6 The effect of particle volume fraction (Φ) on density and magnetization of magnetic fluids

hydrodynamic interaction, there exists the dipolar–dipolar interaction affecting particle relative motion [15]. In low-concentration magnetic fluid samples, magnetic dipolar interactions between magnetic particles are neglected and the magnetic particles in the fluid feel only the external magnetic field fitting the hypothesis of Eq. 4. For higher concentrations, dipolar–dipolar interaction of particles cannot be ignored and this kind of interaction may affect particles' relative motion when magnetized. The interaction between magnetic dipoles increases with the increase of particle concentration and the magnetic moments of part of the particles that are not fully aligned with the magnetic field. The magnetic fluid samples are not yet saturated during the measurement. Due to the wide particle size distribution, part of the nanoparticles is in the single domain range. Thus, the super paramagnetic fraction present in the samples might reduce the magnetization since the magnetic measurements were performed at room temperature. The reasons mentioned above will enlarge the difference between the measured and calculated values.

Conclusions

In this work, the size of ε-Fe_3N nanoparticles was tested by TEM and XRD. Compared with the results, both of the methods are suitable to particle size testing within the experimental error. The amount of surfactant in the fluid seriously affects the stability of magnetic fluid. Stable ε-Fe_3N-based magnetic fluid was prepared by controlling the ratio of carrier liquid and the optimized volume ratio for synthetic oil (PAO4) and surfactant was 4:1. Both the measured and calculated magnetizations increase with increasing particle fraction in the fluid. With the increasing concentration of the ε-Fe_3N particles, the measured values gradually depart from the calculated magnetization, which is caused by the volume fraction and size of the particle agglomeration.

References

1. J.P. Stevenson, M. Rutnakornpituk, M. Vadala, A.R. Esker, S.W. Charles, S. Wells et al., J. Magn. Magn. Mater. **225**, 47–58 (2001). doi:10.1016/S0304-8853(00)01227-0
2. R.Y. Hong, S.Z. Zhang, Y.P. Han, H.Z. Li, J. Ding, Y. Zheng, Powder Technol. **170**, 1–11 (2006). doi:10.1016/j.powtec.2006.08.017
3. H. Mamiya, I. Nakatani, J. Magn. Magn. Mater. **177–181**, 966–967 (1998). doi:10.1016/S0304-8853(97)00572-6
4. L. Vekas, M. Rasa, D. Bica, J. Colloid Interface Sci. **231**, 247–254 (2000). doi:10.1006/jcis.2000.7123
5. S. Odenbach, Colloids Surf. A Physicochem. Eng. Asp. **217**, 171–178 (2003). doi:10.1016/S0927-7757(02)00573-3
6. S. Neveu, A. Bee, M. Robineau, D. Talbot, J. Colloid Interface Sci. **255**, 293–298 (2002). doi:10.1006/jcis.2002.8679
7. M.T.A. Elóia, R.B. Azevedob, E.C.D. Limac, A.C.M. Pimentac, P.C. Morais, J. Magn. Magn. Mater. **289**, 168–170 (2005). doi:10.1016/j.jmmm.2004.11.049
8. B.M. Berkovsky, V.F. Medvedev, M.S. Krakov, *Magnetic Fluids Engineering Applications* (Oxford University Press, 1993)
9. A.E. Berkowitz, J.L. Walter, J. Magn. Magn. Mater. **39**, 75 (1983). doi:10.1016/0304-8853(83)90402-X
10. I. Nakatani, T. Furubayashi, T. Takahashi, H. Hanaoka, J. Magn. Magn. Mater. **65**, 261 (1987). doi:10.1016/0304-8853(87)90046-1
11. I. Nakatani, H. Masayuki, O. Kiyoshi, J. Magn. Magn. Mater. **122**, 10–14 (1993). doi:10.1016/0304-8853(93)91028-6
12. W. Huang, J. Wu, W. Guo, R. Li, L. Cui, J. Magn. Magn. Mater. **307**, 198–204 (2006). doi:10.1016/j.jmmm.2006.03.067
13. C.A. Grimes, D. Qian, E.C. Dickey, J.I. Allen, P.C. Eklund, J. Appl. Phys. **87**, 5642–5644 (2000). doi:10.1063/1.373419
14. J.L. Viota, M. Rasa, S. Sacanna, A.P. Philipse, J. Colloid Interface Sci. **390**, 419–425 (2005)
15. W. Huang, J. Wu, W. Guo, R. Li, L. Cui, Nanoscale Res. Lett. **2**, 155–160 (2007). doi:10.1007/s11671-007-9047-7